Osteoarthritis and Cartilage 27 (2019) 1185–1196

Osteoarthritis and Cartilage

Controlling joint instability after anterior cruciate ligament transection inhibits transforming growth factor-beta-mediated osteophyte formation

K. Murata †, T. Kokubun †, K. Onitsuka ‡, Y. Oka §, T. Kano §, Y. Morishita §, K. Ozone §, N. Kuwabara §, J. Nishimoto §, T. Isho ||, K. Takayanagi †, N. Kanemura † *

† Department of Physical Therapy, School of Health and Social Services, Saitama Prefectural University, Saitama, Japan
‡ Department of Rehabilitation, Tokyo Women's Medical University Yachiyo Medical Center, Chiba, Japan
§ Department of Health and Social Services, Health and Social Services, Graduate School of Saitama Prefectural University, Saitama, Japan
|| Department of Rehabilitation, Fujioka General Hospital, Gunma, Japan

ARTICLE INFO

Article history:
Received 4 June 2018
Accepted 4 March 2019

Keywords:
Knee instability
Osteoarthritis
Smad signaling
Transforming growth factor-beta

SUMMARY

Objective: Abnormal joint instability contributes to cartilage damage and osteophyte formation. We investigated whether controlling joint instability inhibited chronic synovial membrane inflammation and delayed osteophyte formation and examined the role of transforming growth factor-beta (TGF-β) signaling in the associated mechanism.

Design: Rats ($n = 94$) underwent anterior cruciate ligament (ACL) transection. Anterior tibial instability was either controlled (CAM group) or allowed to continue (SHAM group). At 2, 4, and 8 weeks after surgery, radiologic, histopathologic, immunohistochemical, immunofluorescent, and enzyme-linked immunosorbent assay examinations were performed to evaluate osteophyte formation and TGF-β signaling.

Results: Joint instability increased cartilage degeneration score and osteophyte formation, and cell hyperplasia and proliferation and synovial thickening were observed in the synovial membrane. Major findings were increased TGF-β expression and Smad2/3 following TGF-β phosphorylation in synovial membarene, articular cartilage, and the posterior tibial growth plate (TGF-β expression using ELISA: 4 weeks; $P = 0.009$, 95% CI [260.1−1340.0]) (p-Smad2/3 expression density: 4 weeks; $P = 0.024$, 95% CI [1.67−18.27], 8 weeks; $P = 0.034$, 95% CI [1.25−25.34]). However, bone morphogenetic protein (BMP)-2 and Smad1/5/8 levels were not difference between the SHAM model and the CAM model.

Conclusions: This study showed that the difference between anterior tibial instability caused a change in the expression level of TGF in the posterior tibia and synovial membrane, and the reaction might be consequently involved in osteophyte formation.

© 2019 Osteoarthritis Research Society International. Published by Elsevier Ltd. All rights reserved.

Introduction

Mechanical stress is one of the most important factors in the progression of osteoarthritis (OA)[1]. However, the effect of mechanical stress on molecular responses remains unclear. Our previous studies have shown that abnormal joint kinematics is an important mechanical stress factor[2] and that joint instability induces degeneration in the articular cartilage[3]. Consistent with this, clinical studies suggest that self-reported knee instability during the stance phase of gait is associated with significant OA progression[4,5]. Moreover, some patients with OA demonstrate a lateral thrust during walking, and valgus thrust is a major biomechanical risk factor for OA progression[6–8]. Therefore, abnormal joint kinematics and load-induced joint instability might be deeply connected with OA progression, including osteophyte formation and synovitis, in both animal models and humans.

* Address correspondence and reprint requests to: N. Kanemura, Department of Physical Therapy, School of Health and Social Services, Saitama Prefectural University, Saitama, Japan. Tel/Fax: 81-489-73-4123.
E-mail addresses: murata-kenji@spu.ac.jp (K. Murata), kokubun-takanori@spu.ac.jp (T. Kokubun), onikatsuya@yahoo.co.jp (K. Onitsuka), 1981303y@spu.ac.jp (Y. Oka), 1981305a@spu.ac.jp (T. Kano), 1891006q@spu.ac.jp (Y. Morishita), kaichi.ozone@gmail.com (K. Ozone), 1981306q@spu.ac.jp (N. Kuwabara), 1981310a@spu.ac.jp (J. Nishimoto), isho.tak@gmail.com (T. Isho), takayanagi-kiyomi@spu.ac.jp (K. Takayanagi), kanemura-naohiko@spu.ac.jp (N. Kanemura).

https://doi.org/10.1016/j.joca.2019.03.008
1063-4584/© 2019 Osteoarthritis Research Society International. Published by Elsevier Ltd. All rights reserved.

Although osteophytes may help improve instability, osteophyte formation is a clinical characteristic of OA progression. The bone formation changes in osteophyte formation are related to the molecular mechanism of endochondral ossification due to mechanical stress[9]. In recent studies, osteophyte formation has been associated with abnormal mechanical forces that progress in lateral thrust and joint instability conditions and malposition of the meniscus, such as that observed in early OA[10–12]. Moreover, osteophytes exposed to abnormal mechanical stress cause micro-fractures, and the catabolic molecular response causes further progression of OA-related changes[13]. In particular, the molecular response associated with transforming growth factor-beta (TGF-β)/bone morphogenetic protein (BMP) expression can induce osteophytes[14–16]. As a representative example, the signaling pathway induced by TGF-β/BMP includes both Smad-dependent pathway and p38 mitogen-activated protein kinase pathway. Smad signaling in osteophyte formation involves a complex cascade, that is, switching from TGF-β-anaplastic lymphoma kinase (ALK) 5-Smad2/3 signaling to BMP-ALK1-Smad1/5/8 signaling contributes to osteophyte formation and OA pathogenesis[17–19]. The joint structure that plays an important role in these processes is the synovial membrane, and increased nutrients and angiogenesis from the synovial membrane are biological reactions essential for osteophyte formation and endochondral ossification[20,21].

In both humans and animals, osteophytes may develop as a molecular response to joint instability induced by age-related varus or valgus deformities, or abnormal joint mobility after a knee injury. Therefore, some joint instability factors and osteophyte molecular responses might be closely related. We previously developed a novel model for controlled abnormal joint movement, in which the anterior tibia instability induced by an anterior cruciate ligament (ACL) injury was limited using a tightly tied nylon thread[22]. In the traditional ACL tear model, it is unclear whether continued mechanical stress or molecular responses affect OA progression. However, the use of our novel model renders it possible to more clearly evaluate the relationship between joint instability and osteophyte molecular responses in the knee. We found that controlled joint instability inhibited cartilage degeneration and osteophyte formation and suppressed cytokine mediators (e.g., tumor necrosis factor-α and IL-1β) compared to that for continued joint instability. However, detailed changes associated with the relationship between mechanical stress and molecular responses in the synovial membrane, such as those for TGF-β or BMP, are unknown.

In the present study, we evaluated osteophyte progression, osteophyte formation, and cartilage degeneration in the synovial membrane of rats using a widely studied induced instability model of OA and our novel controlled anterior tibial instability (CAM) model. A biochemical analysis was performed to examine the molecular responses in the synovial membrane. We hypothesized that abnormal joint instability, such as those induced by an ACL injury, induce cartilage degeneration and osteophyte formation, and that the osteophyte molecular responses induced by TGF-β-Smad2/3 and BMP-2-Smad1/5 signaling would differ between the evaluated models.

Methods

Animals

Ninety-four 11-week-old Wistar rats (Clea Japan, Tokyo, Japan; weight, 239.3 ± 31.5 g) were randomly assigned to two groups [Fig. 1(A)]. The controlled anterior tibial instability group (CAM) underwent restoration of knee joint kinematics after ACL surgical transection (the anterior tibial joint instability was limited). In the continued anterior tibial instability group (SHAM), the anterior tibial joint instability was induced via traditional ACL surgical transection. After surgery, all rats were housed (2 per cage) and maintained in a room with a 12-hour light–dark cycle and had free access to food and tap water. All procedures were approved by the Ethics Committee of Saitama Prefectural University (approval number: 29-3). In addition, the novel protocol was devised in accordance with the Animal Research: Reporting of *in Vivo* Experiments guidelines.

Surgical procedures

The surgical procedures were as described in our previous study [Fig. 1(B) and (C)][23]. Under a combination anesthetic (medetomidine, 0.375 mg/kg; midazolam, 2.0 mg/kg; and butorphanol, 2.5 mg/kg), the medial capsule of the right knee joint was exposed, without disruption of the patellar tendon, and the ACL was completely transected in both groups. After anterior tibial joint instability was confirmed, both groups underwent the creation of a bone tunnel along the anterior aspect of the proximal tibia, through which a 4-0 nylon thread was passed and tied to the posterior aspect of the distal femur. In the CAM group, the thread was tied tightly, dampening with abnormal joint movement without intra-articular suturing of the ligament (as performed in ACL reconstruction). In contrast, the nylon thread was not tightly tied in the SHAM group, and anterior tibial joint instability remained.

Radiographic evaluation of joint instability

To analyze cartilage degeneration, synovial membrane inflammation, and osteophyte formation, sections of the knee were taken at 4 ($n = 12$) and 8 ($n = 13$) weeks. In accordance with our previous study[2], joint instability was evaluated by anterior traction, using a constant force spring (0.2 kgf), and soft X-ray radiography (M-60; Softex Co., Tokyo, Japan). Soft X-ray radiography was performed at 28 kV and 1 mA for 1 s and was imaged using a NAOMI digital X-ray sensor (RF Co. Ltd., Nagano, Japan). Knee joints were graded from 0 to 4 using our original joint instability score for OA: grade 0, normal contact between the tibia and femur; grade 1 (mild instability), malpositioned meniscus; grade 2 (minimal instability), tibia and femur contact with one-third dehiscence; grade 3 (moderate instability), tibia and femur contact with two-thirds dehiscence; and grade 4 (severe instability), tibia and femur have complete dehiscence. Joint instability was evaluated by two of the authors (Y.O. and T.K.) who were blinded to all other sample information.

At 8 weeks after surgery, the limbs were dissected free of all soft tissues and positioned with 90° flexion at the knee joint to assess OA-related changes. In accordance with our previous study, the frontal and sagittal radiographs were obtained and evaluated by the two authors (T.K. and Y.O.) who were blinded to all other sample information[10,24].

Histological examination

To analyze cartilage degeneration, synovial membrane inflammation, and osteophyte formation, sections of the knee were obtained at 4 weeks ($n = 12$) and 8 weeks ($n = 13$). The knee was fixed in 4% paraformaldehyde for 2 days, and the samples were decalcified in a 10% EDTA-based solution (Sigma–Aldrich, St. Louis, MO, USA) for 40 days. The samples were then embedded in an optimal cutting temperature compound (Sakura FineTek Japan, Tokyo, Japan). The specimens were cut in the sagittal plane (16 μm thickness) using a Leica CM 3050 S cryostat (Leica Microsystems AG, Wetzlar, Germany) and stained with hematoxylin and eosin.

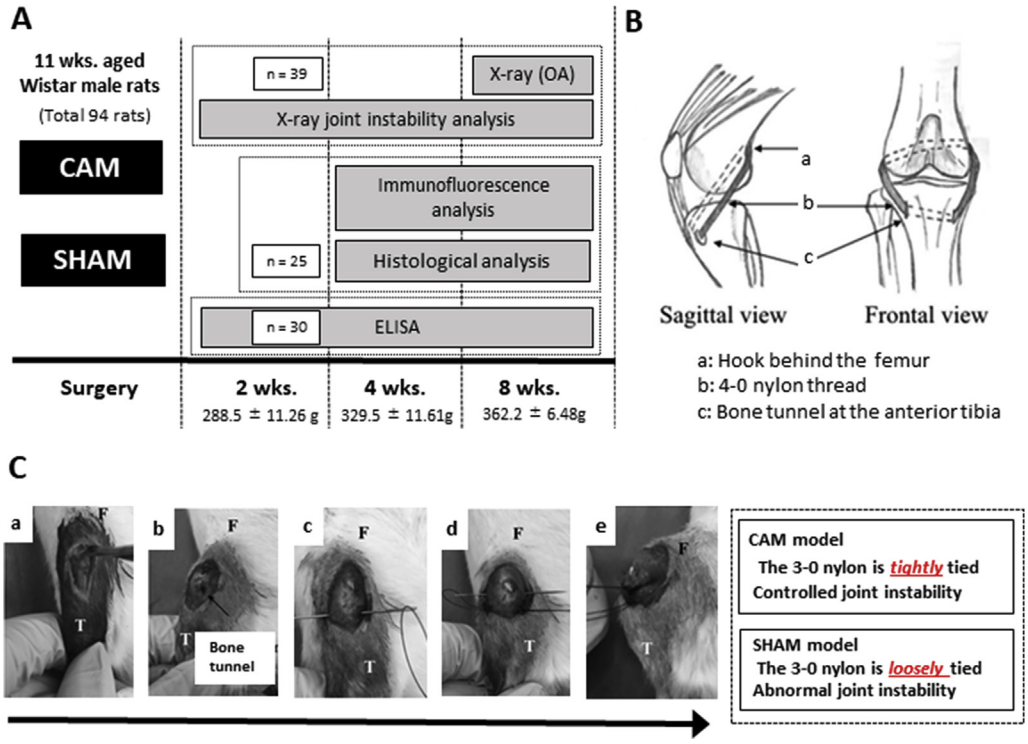

Fig. 1. (A) Study design and timing of the analyses. (B) Schematic representation of the surgical procedure. (C) Surgical protocols for the controlled abnormal joint instability model (CAM group) and continued joint instability model (SHAM group). The models use the same protocol for procedures (a)–(d), but differ in the final procedure (e). Under anesthesia, the right knee joint is exposed via the medial capsule, and the anterior cruciate ligament (ACL) is completely transected (a). After joint instability confirmation, a bone tunnel is created in the anterior portion of the proximal tibia (b). Subsequently, a nylon thread is passed through the tunnel (c) and secured to the posterior aspect of the distal femur (d). To mitigate anterior translation of the tibia on the femur in the CAM group, the nylon thread is placed in the same orientation as the native ACL, providing a posteriorly directed traction force on the tibia that resists anterior motion over the condyles of the femur. In the SHAM model, the 3-0 nylon is loosely tied; therefore, the two models represent different joint instability. F: femur. T: tibia.

Cartilage degeneration was scored using the Mankin system, synovial membrane inflammation was scored using the Osteoarthritis Research Society International (OARSI) scoring system[25], and osteophyte formation was scored as in the study by Little *et al.*[27]. Histological examination was evaluated by two of the authors (Y.O. and T.K.) who were blinded to all other sample information (Supplementary material and methods.).

Immunohistochemical examination

TGF-β, BMP-2, type II collagen, and type I collagen were visualized using the streptavidin-biotin-peroxidase complex technique and semi-quantified as in the study by Santangelo *et al.*[26]. For details, see Supplementary material and methods.

Immunofluorescence examination

In immunofluorescence examination, the sections were incubated overnight at 4°C with rabbit monoclonal anti-p-Smad2/3 antibody (dilution 1:100; #8828, Cell Signaling Technology Japan, Tokyo, Japan) and anti-p-Smad1/5 antibody (dilution 1:200; #9516, Cell Signaling Technology Japan, Tokyo, Japan). Then, they were incubated with goat anti-rabbit-Dylight 488 (dilution 1:200) and counterstained with DAPI (Vector Laboratories, CA, USA). Samples were observed under a BZ-X700 microscope (Keyence, Tokyo, Japan). Immunofluorescent expression density was evaluated for p-Smad2/3 and p-Smad1/5 and quantified using Image J software.

Enzyme-linked immunosorbent assays

At 2, 4, and 8 weeks ($n = 30$, $n = 5$ in each group/time point), total protein samples were prepared by homogenizing the synovial membrane tissue, excluding the meniscus and bone tissue, in a tissue protein extraction reagent (T-PER, Thermo Fisher Scientific, Kanagawa, Japan) containing a protease inhibitor cocktail (Thermo Fisher Scientific). Protein concentrations were determined by using the bicinchoninic acid protein method (Thermo Fisher Scientific). Thereafter, the protein levels of TGF-β (88-50680-22, Thermo Fisher Scientific) and BMP-2 (ab213900, Abcam) were evaluated using Enzyme-linked immunosorbent assay (ELISA) kits in accordance with the manufacturer's instructions.

Statistical analyses

Data were analyzed using SPSS version 25.0 (IBM Japan, Tokyo, Japan) or using R software version 3.5.2. Data were tested for normality and homogeneity using the Shapiro–Wilk test and Levene's test, respectively. For data including time series (2, 4, and 8 weeks), a two-way analysis of variance (ANOVA) or nonparametric two-way ANOVA[28] using the art function in the ARTool package for R according to normality test was used to determine the significant effects of time and surgery (CAM and SHAM) for each parameter. Contrasts were constructed to test for the main effects of grouping (CAM vs SHAM), time (2weeks, 4 weeks and 8 weeks) and their interaction. In the parametric two-way ANOVA, post-hoc test used was the Tukey test or Games–Howell test according to the homogeneity test. In the nonparametric two-way ANOVA,

Mann–Whitney *U* test with Bonferroni-Holm correction was used as a posteriori test. In osteophytes soft X-ray score, the Mann–Whitney *U* test was used to determine differences in osteophyte formation between the CAM and SHAM groups in 8 weeks. Osteophytes histological score was used Welch's test for compare of two group. Parametric data are presented as mean (95% confidence interval: CI), and nonparametric data are presented as median with interquartile ranges [IQR]. Values of $P < 0.05$ were considered statistically significant.

Results

Joint instability analysis

Joint instability data are shown in Fig. 2(A) and (B). The anterior joint instability score was significantly lower in the CAM group than in the SHAM group at 2 weeks (CAM, 1 [range, 0–1]; SHAM, 2.25 [range, 2–3]; $P = 0.005$) and 4 weeks after surgery (CAM, 0 [range, 0–0.75]; SHAM, 1.25 [range, 1–1.5]; $P = 0.008$) [Fig. 2(B)].

Cartilage degeneration and TGF-β and BMP-2 expression in tibial cartilage

The results of the OA analysis are presented in Fig. 3. Cartilage deterioration was observed in the SHAM group at 4 and 8 weeks; in addition to surface fibrillation, cluster cells and cell-free cartilage were observed, with confirmed subchondral bone infiltration. The histological Mankin scores for the knee were significantly higher in the SHAM group than in the CAM group at 4 weeks (33 [30–35] vs 14 [9.5–15.5]; $P = 0.015$) and 8 weeks after surgery (48 [42–51] vs 26 [21–31]; $P = 0.001$).

Representative TGF-β immunostaining of the tibial cartilage is shown in Fig. 3(C) TGF-β expression was significantly higher in the SHAM group than in the CAM group at 4 weeks (14.3 [10.2–18.3] % vs 6.4 [4.8–8.0]%; $P = 0.004$, 95% CI [2.44–13.29]). At 8 weeks, the area of positive staining in a predetermined rectangular area was not significantly higher in the SHAM group than in the CAM group (10.0 [5.8–14.2] % vs 6.5 [4.6–8.5]%; $P = 0.445$, 95% CI [−2.49–9.37]). In contrast, no significant difference in BMP-2 expression was noted between the two groups (4 weeks: CAM, 9.1 [6.5–11.7]%; SHAM, 9.6 [6.9–12.4]%; 8 weeks: CAM, 8.5 [7.1–9.9]%; SHAM, 10.7 [8.4–13.1]%) (Two-way ANOVA main effect; time: $P = 0.858$, group: $P = 0.300$, interaction: $P = 0.505$).

Synovial membrane inflammation score

Microscopic features of the synovial membrane in both groups are shown in Fig. 4. The CAM group had a low number of cell layers and inhibited synovial tissue proliferation compared to those in the SHAM group from 4 to 8 weeks. However, the SHAM group showed tissue thickening, more cell layers, and infiltration of inflammatory cells at 4 weeks; however, the scores of inflammatory findings were not significantly difference at 4 weeks and 8 weeks between the SHAM group and the CAM group (4 weeks: CAM, 1.5 [1–2]; SHAM, 2 [1.5–2.5]; 8 weeks: CAM, 2 [2–3]; SHAM, 4 [3–4]) (4 weeks, $P = 0.093$; 8weeks, $P = 0.138$; post-hoc Mann–Whitney *U* test with Bonferroni-Holm correction).

Chronic synovitis is a finding of OA, with characteristic TGF-β expression. The characteristics of TGF-β immunohistochemical staining were remarkable. At 4 weeks, the thickened synovium was darkly stained and was especially characteristic at the margin where cell infiltration occurred; however, no significant difference was found in the scores between CAM and SHAM groups (4 weeks: CAM, 1.5 [1–2]; SHAM, 2.5 [2–3]; 8 weeks: CAM, 1.5 [1–3]; SHAM, 2 [2–3]) (time; $P = 0.819$, group; $P = 0.050$, interaction; $P = 0.819$: non-parametric two-way ANOVA). The expression of TGF-β was

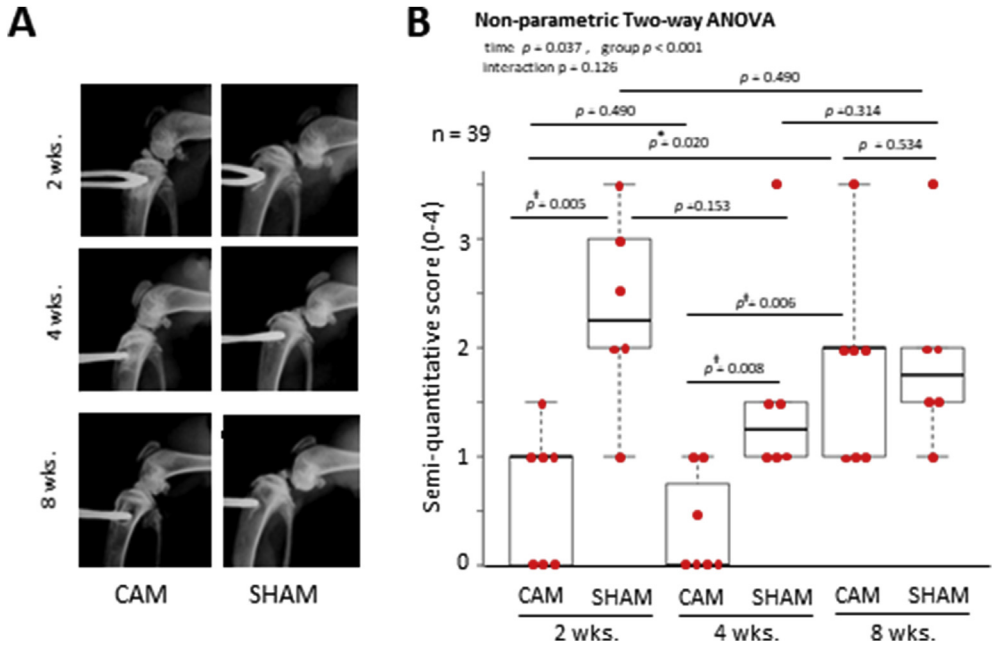

Fig. 2. Joint instability evaluation after surgery. (A) Soft radiographic images for joint instability (sagittal view) evaluated at 2, 4, and 8 weeks after surgery. Anterior translation of the tibia is increased in the SHAM group than in the CAM group. (B) There was a significant main effect for time and group (time: $P = 0.037$, group: $P < 0.001$; non-parametric two-way analysis of variance (ANOVA)). At 2 weeks and 4 weeks, the CAM group has significantly inhibited anterior tibial instability compared to the SHAM group (2 weeks, $P = 0.005$; 4 weeks, $P = 0.008$; post-hoc Mann–Whitney *U* test with Bonferroni-Holm correction); however no significant difference was observed between the SHAM and CAM groups at 8 weeks after surgery ($P = 0.534$; post-hoc Mann–Whitney *U* test with Bonferroni-Holm correction). The kappa coefficient reliability of the two evaluators of joint instability (Y.O. and T.K.) was 0.695. Boxplots show boxes extending from the 25th and 75th percentiles containing the median, with error bars down to the minimum and up to the maximum value. * <0.05, † <0.01.

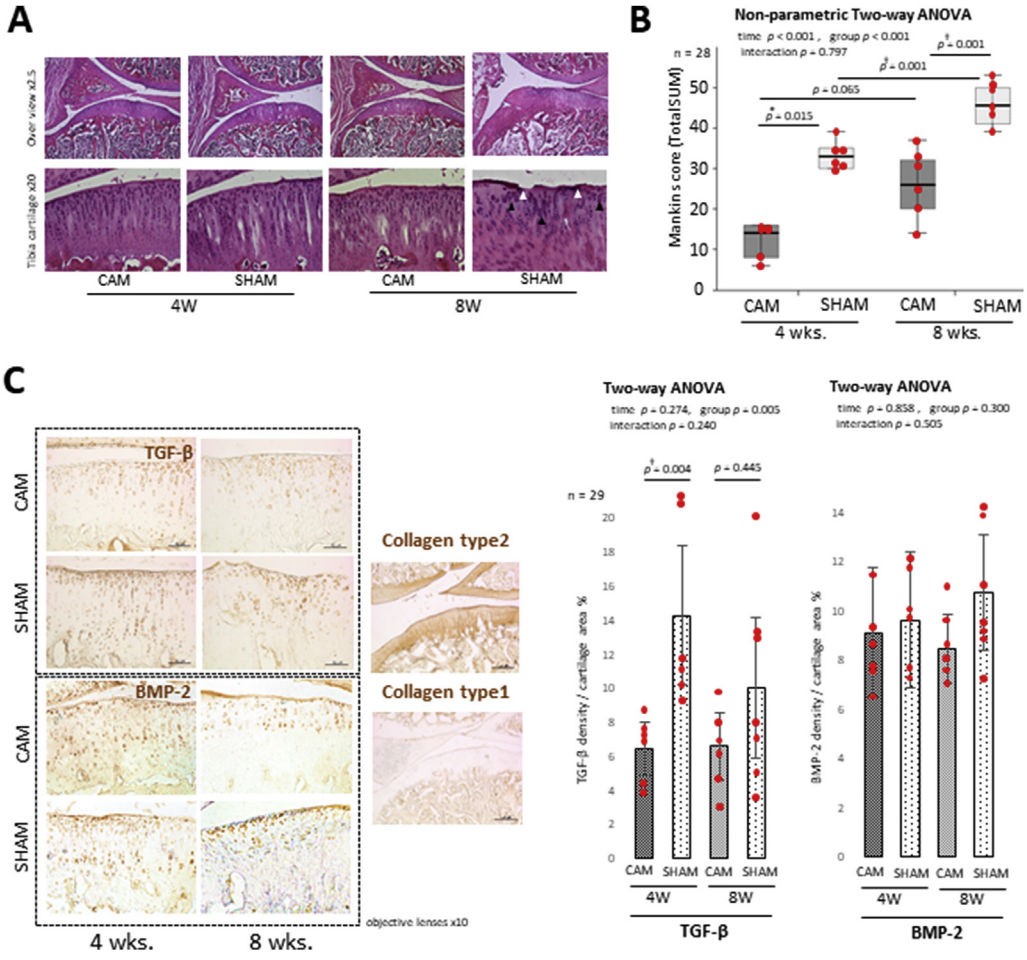

Fig. 3. Controlled abnormal joint movement delayed cartilage degeneration. (A) Histological sections of the cartilage stained with Mayer's hematoxylin and eosin. White arrowheads indicate cartilage pannus and fabrication of the cartilage surface. Black arrowheads indicate cartilage cell proliferation and/or cluster cells. (B) Mankin scores for histological osteoarthritic findings. The CAM group (controlled joint instability model) shows significantly lower score than the SHAM group (continued joint instability model) for the tibia (4 weeks, $P = 0.015$; 8 weeks, $P = 0.001$; post-hoc Mann–Whitney U test with Bonferroni-Holm correction). Boxplots show boxes extending from the 25th and 75th percentiles containing the median, with error bars down to the minimum and up to the maximum value. (C) The CAM section shows decreased TGF-β, bone morphogenetic protein (BMP)-2, and collagen type 2 and type 1 for positive control in the articular cartilage compared to that in the SHAM section at 8 weeks after surgery. In TGF-β, the semi-quantitative score for the tibia is significantly higher in the SHAM group than in the CAM group at 4 weeks (4 weeks, $P = 0.004$; post-hoc Games–Howell test); however no significant difference was observed between the SHAM and CAM groups at 8 weeks after surgery ($P = 0.445$; post-hoc Games–Howell test). Data are presented as means and 95% CIs. FA, femur anterior; FP, femur posterior; TA, tibia anterior; TP, tibia posterior; * <0.05, † <0.01.

higher in the cell-infiltrated area than in the non-infiltrated area, in contrast to that observed on hematoxylin and eosin staining. BMP-2 expression was not significant between the two groups at 4 and 8 weeks (4 weeks: CAM, 1.5 [1–2]; SHAM, 2.5 [2–3]; 8 weeks: CAM, 1 [1-1]; SHAM, 1 [1–2]) (time; $P = 0.149$, group; $P = 0.109$, interaction; $P = 0.343$: non-parametric two-way ANOVA).

TGF-β and BMP protein expression using ELISA

Fig. 5 shows the TGF-β and BMP-2 protein expression values obtained from the synovial membrane samples. The group difference at 8 weeks after surgery was not statistically significant (8 weeks: CAM, 811.9 [670.6–953.2] pg/mL; SHAM, 585.3 [396.2–774.4] pg/mL; $P = 0.131$, 95% CI [−84.0–537.1]). At 2 weeks after surgery, TGF-β expression in the synovium was significantly increased in the CAM group than in the SHAM group (2 weeks: CAM, 3177.0 [2589.3–3764.7] pg/mL; SHAM, 2131.4 [1623.0–2639.8] pg/mL; $P = 0.046$, 95% CI [23.4–2067.7].); however, 4 weeks after surgery, TGF-β expression in the synovium was significantly decreased in the CAM group than in the SHAM group (4 weeks: CAM, 868.9 [696.9–1040.9] pg/mL; SHAM, 1668.9 [1296.2–2041.7] pg/mL; $P = 0.009$, 95% CI [260.1–1340.0]). The BMP expression has no statistically significant difference between the CAM and SHAM groups at 2, 4, and 8 weeks after surgery (2 weeks: CAM, 62.6 [44.3–80.9] pg/mL; SHAM, 107.6 [57.8–157.4] pg/mL) (4 weeks: CAM, 58.4 [41.8–74.9] pg/mL; SHAM, 51.0 [39.7–62.2] pg/mL) (8 weeks: CAM, 43.4 [32.3–54.4] pg/mL; SHAM, 52.4 [47.8–57.1] pg/mL]) (Two-way ANOVA main effect: time; $P = 0.190$, group; $P = 0.231$, interaction; $P = 0.149$).

Osteophyte radiographic and histological examinations

On radiographic assessment, knee features were mostly categorized as grade 2 or 3 at 8 weeks after surgery [Fig. 6(A)]. Grading scale scores were significantly higher in the SHAM group than in the CAM group (1.5 [1–2] vs 0.5 [0–0.5]; $P = 0.009$). The osteophyte score [Fig. 6(B)] was significantly lower in the CAM group than in the SHAM group at 8 weeks after surgery (total: CAM, 6.0 [4.4–7.6]; SHAM, 12.3 [11.3–13.3]; $P < 0.001$, 95% CI [3.67–8.52]). Sub score was also statistically significant difference in size and maturity

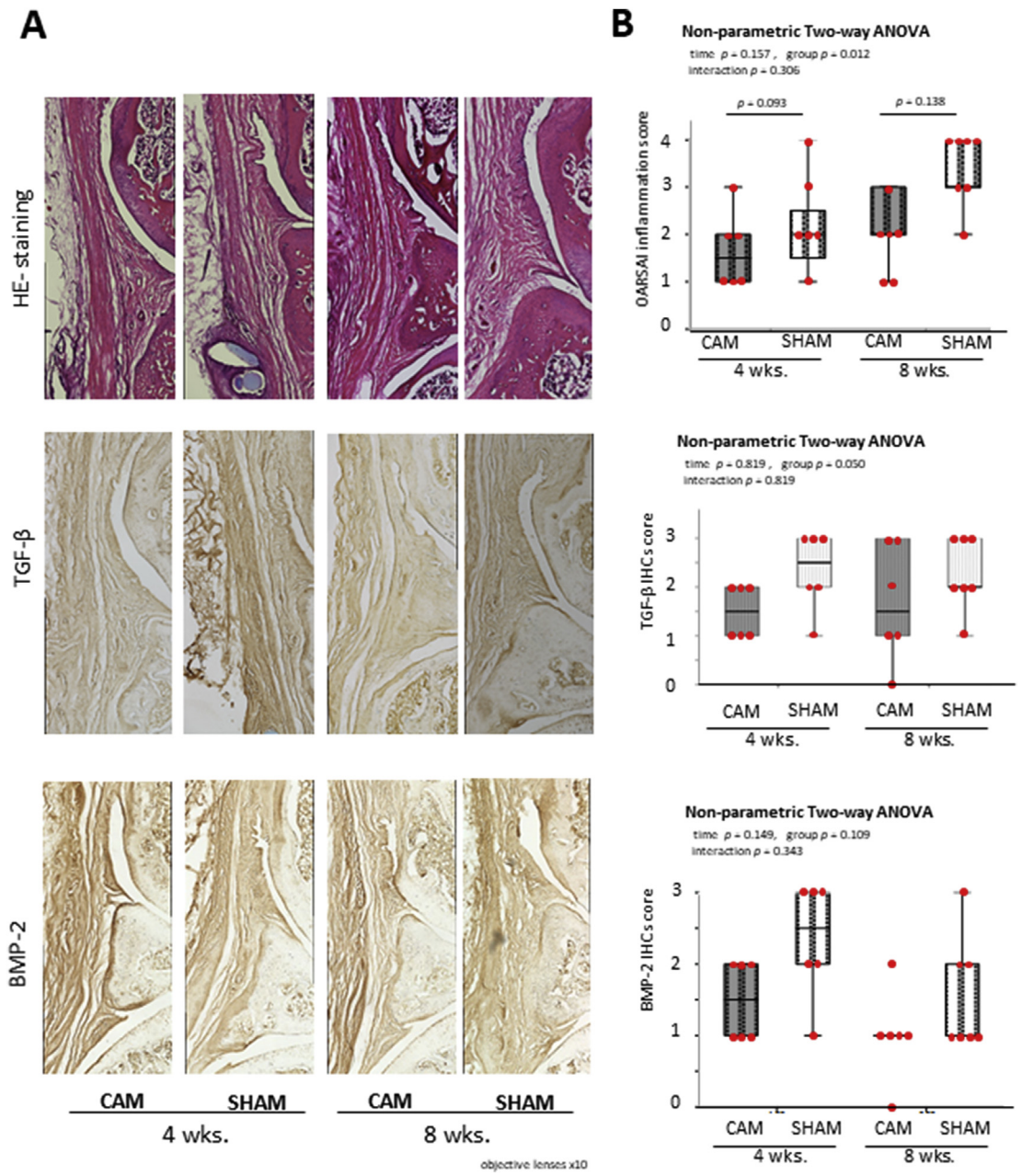

Fig. 4. Controlled abnormal joint movement shows inhibited synovial membrane inflammation and synovial thickening, TGF-β and BMP-2 IHC staining. (A) Histological sections of the synovial membrane stained using Mayer's hematoxylin and eosin. (B) The histological synovial inflammation scores and IHC staining scores were indicated. There was a significant main effect for group ($P = 0.012$; non-parametric two-way ANOVA); however no significant difference was observed between the SHAM and CAM groups at 4 weeks and 8 weeks after surgery (4 weeks, $P = 0.093$; 8weeks, $P = 0.138$; post-hoc Mann–Whitney *U* test with Bonferroni-Holm correction). TGF-β scores were not significantly higher in the CAM model than in the SHAM model (time, $P = 0.819$; group, $P = 0.050$; interaction, $P = 0.819$; non-parametric two-way ANOVA). BMP-2 expression was not significant difference between the two groups at 4 weeks and 8 weeks (time, $P = 0.149$; group, $P = 0.109$; interaction, $P = 0.343$; non-parametric two-way ANOVA). Boxplots show boxes extending from the 25th and 75th percentiles containing the median, with error bars down to the minimum and up to the maximum value. HE, hematoxylin and eosin; MM, medial meniscus; TGF-β, transforming growth factor-beta.

between the two groups (maturity: CAM, 2.17 [1.62–2.72]; SHAM, 5.14 [4.4–5.9]; $P < 0.001$, 95% CI [1.67–4.13]) (size: CAM, 3.83 [2.8–4.9]; SHAM, 7.1 [6.3–8.0]; $P = 0.001$, 95% CI [1.45–4.92]).

Smad2/3 expression on immunofluorescence analysis

P-Smad2/3 and P-Smad1/5 expression in the cartilage metaplasia area was increased to a greater extent in the SHAM group than in the CAM group [Fig. 7(A)], consistent with the pattern of results for TGF-β staining. P-Smad2/3 density was markedly upregulated in the SHAM group than in the CAM group at 4 weeks (CAM, 16.1 [12.1–20.0]%; SHAM, 26.9 [22.2–31.5]%; $P = 0.024$, 95% CI [1.67–18.27]) and 8 weeks after surgery (CAM, 17.6 [10.8–24.4]%; SHAM, 33.7 [27.8–39.6]%; $P = 0.034$, 95% CI [1.25–25.34]). P-Smad1/5 density was not significantly upregulated in the SHAM group than in the CAM group at 4 weeks and 8 weeks (4weeks: 21.3 [13.7–29.0]% vs 17.3 [12.5–23.2]%; $P = 0.471$, 8weeks: CAM, 15.1 [8.4–21.8]%; SHAM, 24.8 [17.7–31.9]%; $P = 0.136$).

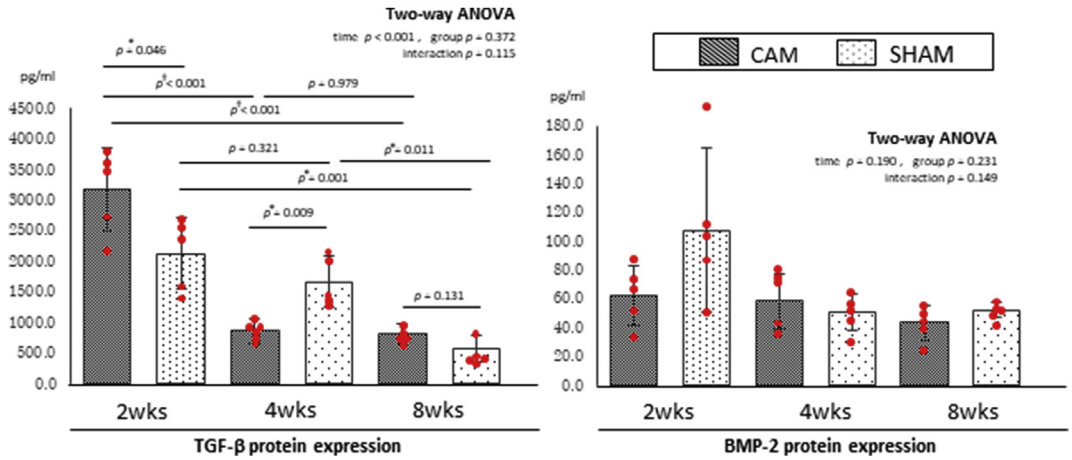

Fig. 5. ELISA results for TGF-β and BMP-2 expression levels in the synovial membrane. At 2 weeks after surgery, TGF-β levels are lower in the SHAM group than in the CAM group ($n = 5$ in each group; 2 weeks, $P = 0.046$); however, at 4 weeks after surgery, TGF-β levels are lower in the CAM group than in the SHAM group ($n = 5$ in each group; 4 weeks, $P = 0.009$). At 8 weeks after surgery no difference was found between the SHAM and CAM groups ($n = 5$ in each group; 8 weeks, $P = 0.131$). For BMP-2 levels, the groups show no significant difference at any time point (time, $P = 0.190$; group, $P = 0.231$, interaction, $P = 0.149$; two-way ANOVA). Data are presented as means and 95% CIs. BMP-2, BMP; CI, confidence interval; TGF-β, transforming growth factor-beta.

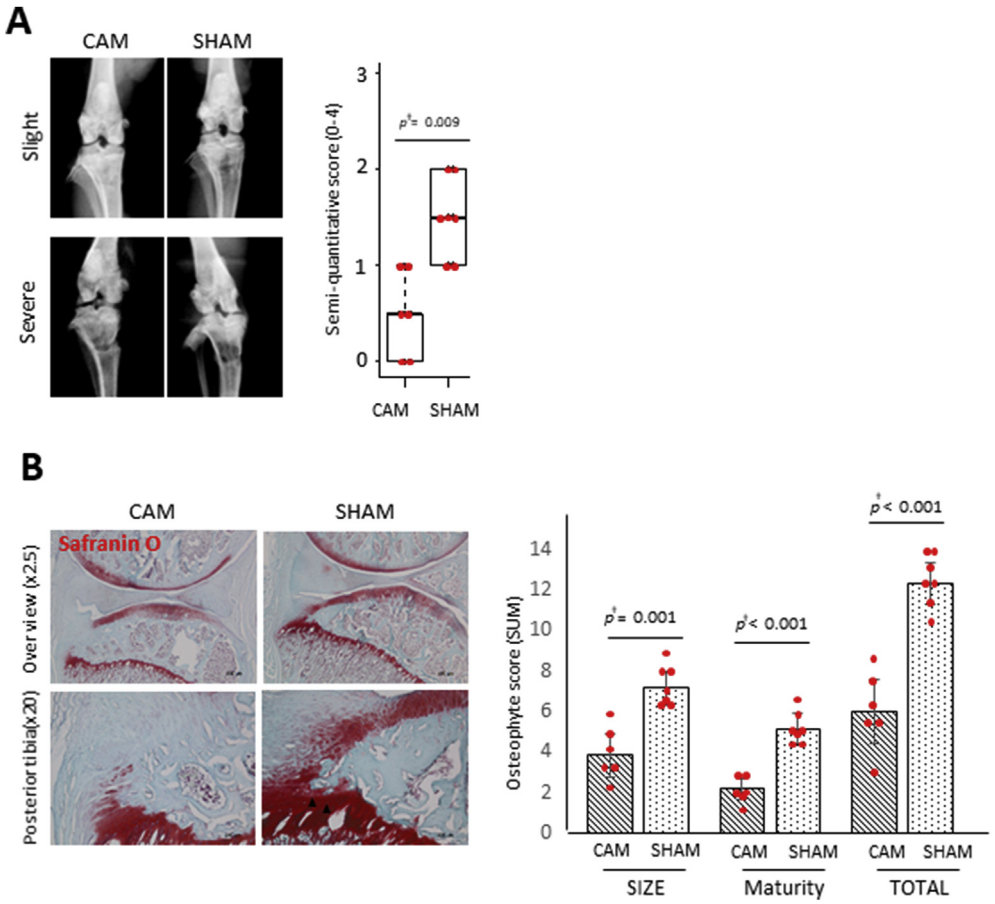

Fig. 6. Controlled abnormal joint movement inhibits osteophyte formation. (A) Soft radiographic images of osteophyte formation (frontal view) in the CAM and SHAM groups at 8 weeks after surgery. The semi-quantitative scores show significant increase in the SHAM group than in the CAM group (8 weeks, $P = 0.009$; Mann–Whitney U test). Boxplots show boxes extending from the 25th and 75th percentiles containing the median, with error bars down to the minimum and up to the maximum value. (B) Histological sections of the tibia posterior stained using Safranin O/fast green stains. Black arrowheads indicate chondroid metaplasia and osteophyte formation in the posterior tibia. Histological osteophyte formation scores. The CAM group shows significantly inhibited osteophyte size score and total score compared to those in the SHAM group (size score, $P = 0.002$; mature score, $P < 0.001$; total score, $P < 0.001$; Welch's t test). Data are presented as means and 95% CIs.

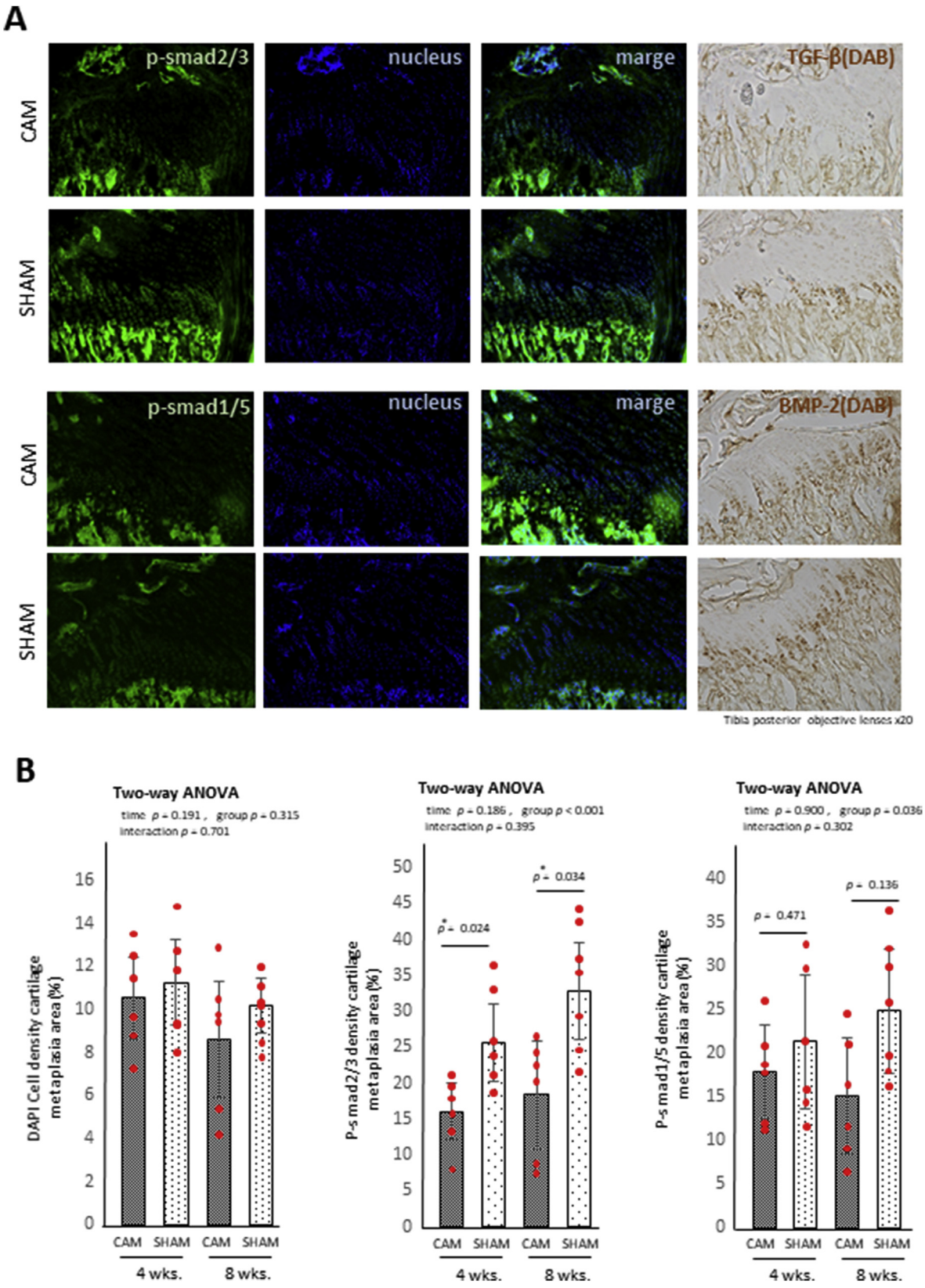

Fig. 7. Controlled abnormal joint movement inhibits p-Smad2/3 expression in cartilage metaplasia. (A) Immunofluorescence sections for anti-p-Smad2/3 and TGF-β, anti-p-Smad1/5/8 and BMP-2. The square area indicates the overexpression of p-Smad2/3 in cartilage metaplasia. TGF-β is also expressed in the same area. (B) Immunofluorescent density scores for p-Smad2/3, p-Smad1/5, and the nucleus. The CAM group has a significantly inhibited cartilage metaplasia score compared to that in the SHAM group at 4 and 8 weeks after surgery (4 weeks, $P = 0.024$; 8 weeks, $P = 0.034$; post-hoc Tukey test). p-Smad1/5 was markedly upregulated in the SHAM group than in the CAM group (4 weeks, $P = 0.471$; 8 weeks, $P = 0.135$; post-hoc Tukey test) and 8 weeks after surgery. Data are presented as means and 95% CIs. CI, confidence interval; TGF-β, transforming growth factor-beta.

Discussion

We investigated TGF-β and BMP-2 signaling in two different joint instability models reflecting different aspects of human OA. Controlling joint instability after ACL injury decreased TGF-β1 and Smad2/3 expression and inhibited synovial cell hyperplasia and proliferation in the long term. As a result, osteophyte formation and cartilage degeneration were inhibited in the knee joint.

Experimental knee OA model based on the generation of joint instability (induced by ACL transection) shares some important features with human OA, including the development of osteophytes and cartilage erosions. In particular, cartilage degeneration and osteophyte formation, induced by mechanical stress, are important features common to human OA and experimental OA in animals. Furthermore, the conversion of appropriate mechanical stress to biochemical responses is an important factor for maintaining cartilage structure, function, and cells. However, excessive mechanical stress results in the deterioration in the homeostasis of various tissues and triggers cartilage degeneration, chondrophyte/osteophyte formation, and sclerosis of the subchondral bone in the knee joint. In previous studies, joint instability[29], varus thrust during ambulation[30,31], and cartilage overload and trauma[32,33] have been reported as the main mechanical stress factors in OA. We believe that controlling mechanical stress can contribute to OA prevention. The knee joint, which is anatomically an unstable bone structure, maintains stability via the ligament and meniscus. Therefore, the destabilization of the medial meniscus[34] model and the ACL transection model[35] are common OA models induced by joint instability, and the models promote osteophyte formation, as well as cartilage degeneration[36]. Therefore, we hypothesized that this abnormal mechanical stress was involved in the instability of the joints.

We focused on knee instability and developed a model to control the instability of the joint after injury to the ligament. Using the model, our previous study was able to demonstrate suppression of degeneration of the cartilage and promotion of ACL repair in rats[2,22]. The joint kinematics maintains the appropriate mobility and stability during movements, such as rolling and sliding[37]. Repeated abnormal joint movements, leading to arthritis and pain, are common clinical responses of joint instability due to damage or structural abnormalities present in large joints, such as the knee, shoulder, and hip joints. Although the patients with knee OA symptoms report joint instability, joint mechanics in OA patients resembled those in stable OA patients[38]. Therefore, this might indicate that more detailed intra-articular joint movements and contact mechanics might lead to altered joint contact stresses and cause articular cartilage damage. Histological analysis of our data revealed more pronounced changes, such as cartilage degeneration and osteophyte formation, between the two groups due to joint instability.

Osteophyte formation induced by endochondral ossification is necessary for various molecular mechanisms caused by mechanical stress. The synovial membrane, located at the margin of the joint, is an important tissue in osteophyte formation in knee OA, because it contributes to vascular supply necessary for bone formation. The histological pattern of the synovium in patients with OA is characterized by the proliferation of synovial tissue, infiltration of fibrosis and macrophages, and hyperplasia of the lining. Macrophages in the synovial membrane increase the production of inflammatory mediators and immune cells after increasing angiogenesis. A vicious cycle follows as tissues produce additional cytokines and proteolytic enzymes that further induce synovial inflammation and eventually increase cartilage degradation. Therefore, chronic inflammatory findings in synovial membranes have various roles, such as angiogenesis and expression of pain.

As a molecular response example, expression of TGF superfamily in the synovial membrane is greatly involved in osteophyte formation and includes TGF-β1 and BMP-2. These factors play an important role in cell proliferation, differentiation, and apoptosis control[39]. TGF-β1 and BMP-2 in the cartilage and synovial membrane were reported to promote the formation of osteochondral bone, suggesting that factors are involved in osteophyte formation in OA[40]. Several reports have promoted the formation of osteophytes by injecting TGF in the joints[41]; therefore, TGF-β1 is a main factor for osteophyte formation. In addition, TGF-β and BMP-2 bind to the receptor, such ALK-1 or ALK-5, and phosphorylate the Smad protein present in cells to transmit signals[21]. Specifically, in the TGF-β/activin pathway, TGF-β binds to the receptor ALK-1, and signaling is initiated by the phosphorylation of Smad2/3. In contrast, BMP-2 binds to the receptor ALK-5, and signaling is initiated by the phosphorylation of Smad1/5. In the present study, the early control of joint instability suppressed the thickening of the synovial tissue and delayed the invasion of the synovial cells. Moreover, the change in mechanical stress clearly altered the biochemical responses of TGF-β or Smad2/3 at 4 weeks' time point. However, BMP-2 and Smad1/5/8 levels were not difference between the SHAM model and the CAM model. This indicated that early control of joint instability inhibited the signaling pathway of bone formation associated in TGF-β (Fig. 8).

The relation between mechanical stress and osteophyte is induced by the accumulated mechanical stress, but information about the underlying molecular mechanism is limited. Kawaguchi *et al.* showed that the internal ossification process found in the growth plate cartilage, such as hypertrophic differentiation/apoptosis of chondrocytes, is induced by mechanical stress. At the joint margin where the blood vessels can invade the synovium, intra-cartilage ossification occurs, and osteophytes are formed. Although there are many unclear points about the specific type of mechanical stress, the relevance of joint instability and osteophytes has been reported. A mechanical stimulus possibly caused by joint instability has been converted to a biochemical signal causing endochondral ossification. Since their bone spurs proliferate in response to experimentally induced instability, their formation can

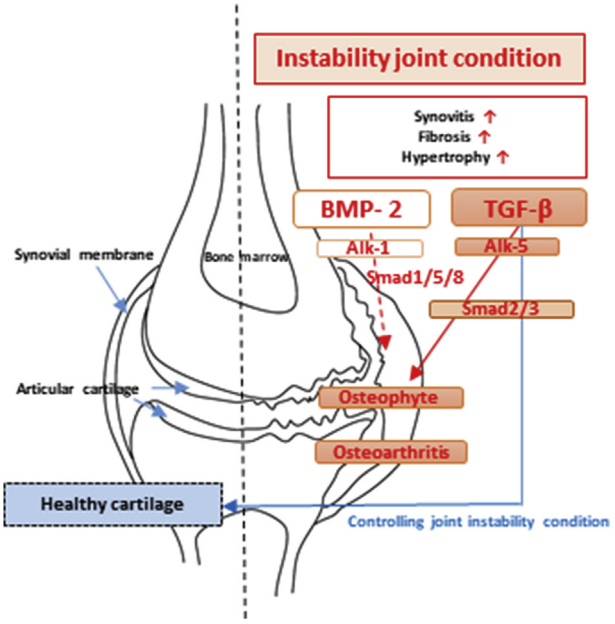

Fig. 8. Transforming growth factor-beta family and joint instability strategy for osteoarthritis cartilage and osteophyte formation.

be seen as mechanical adaptability (restoring stability) rather than degeneration. In particular instances, osteophytes contribute to joint stability, although they may restrict the range of motion.

The present study has some limitations that should be acknowledged. The restoration of natural joint kinematics requires the static articulation of joint instability. The use of an experimental OA rat model implies a small size; thus, changes in the dynamic joint kinematics (including tibial rotation) following ACL transection could not be accurately evaluated. It is not easy to accurately and mechanically measure this dynamic instability, and it is difficult to define normalization/abnormality of joint movement. Rodent models have become popular for assessing the consequences of OA[42]. Our biomechanics group is working on the ability to evaluate dynamic instability; however, additional time is necessary. Gait analyses might be included in our next animal study. Second, in this study, ACL transection and CAM surgery were done at the same time. In humans, ACL injury and repair are separated by several weeks, and the repair surgery is a "second insult" on the joint. In this respect, there might be considerable differences between the animal model and the human condition. Third, in this study, we have not verified ALK (activin-like kinase) 2, ALK 3, ALK 6 as type I receptor (ALK 5) activated by binding with TGF-β, and type I receptor of BMP. ALK phosphorylates the Smad protein and has an important function of transmitting a signal into the cell. Therefore, in this study, the quantitative change in TGF and BMP and the complicated process in the change in ALK are insufficient.

Importantly, this study showed that the difference between the anterior tibial instability causes a change in the expression level of TGF in the posterior growth plate and synovial membrane, and the reaction might be consequently involved in osteophyte formation (Fig. 8). Clinically, bone formation is a general characteristic of OA. Although advanced OA changes accompany severe osteophyte formation, it is only one of the responses in basic OA progression. Considering that joint instability (as lateral thrust) promotes cartilage degeneration and many patients with OA present with joint anxiety, the formation of osteophytes may be favorable for the instability. However, an increase in osteophytes is an indicator of OA progression in knee joint inflammation, accompanied by fine fractures in the Kellgren–Lawrence classification system, and it can be considered an abnormal change. Future studies must determine the need for suppression of osteophyte formation.

Author contributions

All authors have read and approved the final submitted manuscript.

Study design: K. Murata.

Surgery and surgical assistance: K. Murata, K. Onitsuka, Y. Oka, and T. Kano.

Data collection: K. Murata. K. Onitsuka, Y. Oka, T. Kano, Kuwabara, and J. Nishimoto.

Histological analysis: K. Murata., Y. Oka, and T. Kano, Y. Morishita, and K. Ozone.

Radiography evaluation: K. Murata., Y. Oka, and T. Kano.

Manuscript composition: K. Murata, T. Kokubun, and N. Kanemura.

Funding: K. Murata, T. Kokubun, T. Takayanagi, and N. Kanemura.

Statistical analysis: K. Murata, T. Isho.

Conflict of interest

None of the authors have a conflict of interest related to the manuscript.

Role of the funding source

This study was supported by a JSPS KAKENHI (17K17984) Grant-in-Aid for Young Scientists (B).

Acknowledgment

The authors thank Yuki Minegishi (Houei Hospital, PT) and Mitsuhiro Kameda (Kasukabe Chuo General Hospital) for their assistance with the surgery and sample collection. They also thank Namine Kiso, Kanae Mastui, Shiori Tsukamoto, and Yoko Shirose (students at Saitama Prefectural University) for their assistance with the surgery and sample collection.

Supplementary data

Supplementary data to this article can be found online at https://doi.org/10.1016/j.joca.2019.03.008.

References

1. Buckwalter JA, Anderson DD, Brown TD, Tochigi Y, Martin JA. The roles of mechanical stresses in the pathogenesis of osteoarthritis. Cartilage 2013;4:286–94, https://doi.org/10.1177/1947603513495889.
2. Murata K, Kanemura N, Kokubun T, Fujino T, Morishita Y, Onitsuka K, *et al*. Controlling joint instability delays the degeneration of articular cartilage in a rat model. Osteoarthritis Cartilage 2017;25:297–308, https://doi.org/10.1016/j.joca.2016.10.011.
3. Allen KD, Mata BA, Gabr MA, Huebner JL, Adams Jr SB, Kraus VB, *et al*. Kinematic and dynamic gait compensations resulting from knee instability in a rat model of osteoarthritis. Arthritis Res Ther 2012;14:R78, https://doi.org/10.1186/ar3801.
4. Knoop J, van der Leeden M, van der Esch M, Thorstensson CA, Gerritsen M, Voorneman RE, *et al*. Association of lower muscle strength with self-reported knee instability in osteoarthritis of the knee: results from the Amsterdam Osteoarthritis Cohort. Arthritis Care Res 2012;64:38–45, https://doi.org/10.1002/acr.20597.
5. Gustafson JA, Gorman S, Fitzgerald GK, Farrokhi S. Alterations in walking knee joint stiffness in individuals with knee osteoarthritis and self-reported knee instability. Gait Posture 2016;43:210–5, https://doi.org/10.1016/j.gaitpost.2015.09.025.
6. Lewek MD, Rudolph KS, Snyder-Mackler L. Control of frontal plane knee laxity during gait in patients with medial compartment knee osteoarthritis. Osteoarthritis Cartilage 2004;12:745–51, https://doi.org/10.1016/j.joca.2004.05.005.
7. Sharma L, Hurwitz DE, Thonar EJ, Sum JA, Lenz ME, Dunlop DD, *et al*. Knee adduction moment, serum hyaluronan level, and disease severity in medial tibiofemoral osteoarthritis. Arthritis Rheum 1998;41:1233–40.
8. Baliunas AJ, Hurwitz DE, Ryals AB, Karrar A, Case JP, Block JA, *et al*. Increased knee joint loads during walking are present in subjects with knee osteoarthritis. Osteoarthritis Cartilage 2002;10:573–9, https://doi.org/10.1053/joca.2002.0797.
9. Kawaguchi H. Endochondral ossification signals in cartilage degradation during osteoarthritis progression in experimental mouse models. Mol Cell 2008;25:1–6.
10. Murata K, Kokubun T, Morishita Y, Onitsuka K, Fujiwara S, Nakajima A, *et al*. Controlling abnormal joint movement inhibits response of osteophyte formation. Cartilage 2017, https://doi.org/10.1177/1947603517700955. 194760351770095.
11. Hada S, Ishijima M, Kaneko H, Kinoshita M, Liu L, Sadatsuki R, *et al*. Association of medial meniscal extrusion with medial tibial osteophyte distance detected by T2 mapping MRI in patients with early-stage knee osteoarthritis. Arthritis Res

Ther 2017;19:1–12, https://doi.org/10.1186/s13075-017-1411-0.
12. Hunter DJ, Zhang YQ, Niu JB, Tu X, Amin S, Clancy M, *et al*. The association of meniscal pathologic changes with cartilage loss in symptomatic knee osteoarthritis. Arthritis Rheum 2006;54:795–801, https://doi.org/10.1002/art.21724.
13. Liu-Bryan R, Terkeltaub R. Emerging regulators of the inflammatory process in osteoarthritis. Nat Rev Rheumatol 2015;11:35–44, https://doi.org/10.1038/nrrheum.2014.162.
14. Blaney Davidson EN, Vitters EL, van Beuningen HM, van de Loo FAJ, van den Berg WB, van der Kraan PM. Resemblance of osteophytes in experimental osteoarthritis to transforming growth factor β-induced osteophytes: limited role of bone morphogenetic protein in early osteoarthritic osteophyte formation. Arthritis Rheum 2007;56:4065–73, https://doi.org/10.1002/art.23034.
15. van Beuningen HM, Glansbeek HL, van der Kraan PM, van den Berg WB. Differential effects of local application of BMP-2 or TGF-beta 1 on both articular cartilage composition and osteophyte formation. Osteoarthritis Cartilage 1998;6:306–17, https://doi.org/10.1053/joca.1998.0129.
16. Keller B, Yang T, Chen Y, Munivez E, Bertin T, Zabel B, *et al*. Interaction of TGFβ and BMP signaling pathways during chondrogenesis. PLoS One 2011;6:e16421, https://doi.org/10.1371/journal.pone.0016421.
17. van der Kraan PM, Blaney Davidson EN, van den Berg WB. A role for age-related changes in TGFbeta signaling in aberrant chondrocyte differentiation and osteoarthritis. Arthritis Res Ther 2010;12:201, https://doi.org/10.1186/ar2896.
18. van der Kraan PM, Blaney Davidson EN, Blom A, van den Berg WB. TGF-beta signaling in chondrocyte terminal differentiation and osteoarthritis. Modulation and integration of signaling pathways through receptor-Smads. Osteoarthritis Cartilage 2009;17:1539–45, https://doi.org/10.1016/j.joca.2009.06.008.
19. Blaney Davidson EN, Vitters EL, van der Kraan PM, van den Berg WB. Expression of transforming growth factor-beta (TGFbeta) and the TGFbeta signaling molecule SMAD-2P in spontaneous and instability-induced osteoarthritis: role in cartilage degradation, chondrogenesis and osteophyte formation. Ann Rheum Dis 2006;65:1414–21, https://doi.org/10.1136/ard.2005.045971.
20. Kaneko H, Ishijima M, Futami I, Tomikawa-Ichikawa N, Kosaki K, Sadatsuki R, *et al*. Synovial perlecan is required for osteophyte formation in knee osteoarthritis. Matrix Biol 2013;32:178–87, https://doi.org/10.1016/j.matbio.2013.01.004.
21. Shen J, Li S, Chen D. TGF-β signaling and the development of osteoarthritis. Bone Research 2014;2:14002, https://doi.org/10.1038/boneres.2014.2.
22. Kokubun T, Kanemura N, Murata K, Moriyama H, Morita S, Jinno T, *et al*. Effect of changing the joint kinematics of knees with a ruptured anterior cruciate ligament on the molecular biological responses and spontaneous healing in a rat model. Am J Sports Med 2016;44:2900–10, https://doi.org/10.1177/0363546516654687.
23. Murata K, Kanemura N, Kokubun T, Morishita Y, Fujino T, Takayanagi K. Acute chondrocyte response to controlling joint instability in an osteoarthritis rat model. Sport Sci Health 2016;13:113–9, https://doi.org/10.1007/s11332-016-0320-y.
24. Oprenyeszk F, Chausson M, Maquet V, Dubuc JE, Henrotin Y. Protective effect of a new biomaterial against the development of experimental osteoarthritis lesions in rabbit: a pilot study evaluating the intra-articular injection of alginate-chitosan beads dispersed in an hydrogel. Osteoarthritis Cartilage 2013;21:1099–107, https://doi.org/10.1016/j.joca.2013.04.017.
25. Gerwin N, Bendele AM, Glasson S, Carlson CS. The OARSI histopathology initiative - recommendations for histological assessments of osteoarthritis in the rat. Osteoarthritis Cartilage 2010;18:S24–34, https://doi.org/10.1016/j.joca.2010.05.030.
26. Santangelo KS, Pieczarka EM, Nuovo GJ, Weisbrode SE, Bertone AL. Temporal expression and tissue distribution of interleukin-1β in two strains of Guinea pigs with varying propensity for spontaneous knee osteoarthritis. Osteoarthritis Cartilage 2011;19:439–48, https://doi.org/10.1016/j.joca.2011.01.004.
27. Little CB, Barai A, Burkhardt D, Smith SM, Fosang AJ, Werb Z, *et al*. Matrix metalloproteinase 13-deficient mice are resistant to osteoarthritic cartilage erosion but not chondrocyte hypertrophy or osteophyte development. Arthritis Rheum 2009;60:3723–33, https://doi.org/10.1002/art.25002.
28. Wobbrock JO, Findlater L, Gergle D, Higgins JJ. The Aligned Rank Transform for Nonparametric Factorial Analyses Using Only ANOVA Procedures. ACM Press; 2011143–6.
29. Kamekura S, Hoshi K, Shimoaka T, Chung U, Chikuda H, Yamada T, *et al*. Osteoarthritis development in novel experimental mouse models induced by knee joint instability. Osteoarthritis Cartilage 2005;13:632–41, https://doi.org/10.1016/j.joca.2005.03.004.
30. Chang A, Hayes K, Dunlop D, Hurwitz D, Song J, Cahue S, *et al*. Thrust during ambulation and the progression of knee osteoarthritis. Arthritis Rheum 2004;50:3897–903, https://doi.org/10.1002/art.20657.
31. Sharma L, Chang AH, Jackson RD, Nevitt M, Moisio KC, Hochberg M, *et al*. Varus thrust and incident and progressive knee osteoarthritis. Arthritis Rheumatology 2017;69:2136–43, https://doi.org/10.1002/art.40224.
32. Wink AE, Gross KD, Brown CA, Guermazi A, Roemer F, Niu J, *et al*. Varus thrust during walking and the risk of incident and worsening medial tibiofemoral MRI lesions: the Multicenter Osteoarthritis Study. Osteoarthritis Cartilage 2017;25:839–45, https://doi.org/10.1016/j.joca.2017.01.005.
33. Onur TS, Wu R, Chu S, Chang W, Kim HT, Dang AB. Joint instability and cartilage compression in a mouse model of posttraumatic osteoarthritis. J Orthop Res 2014;32:318–23, https://doi.org/10.1002/jor.22509.
34. Glasson SS, Blanchet TJ, Morris EA. The surgical destabilization of the medial meniscus (DMM) model of osteoarthritis in the 129/SvEv. Osteoarthritis Cartilage 2007;15:1–1069, https://doi.org/10.1016/j.joca.2007.03.006.
35. McCoy AM. Animal models of osteoarthritis: comparisons and key considerations. Veterinary Pathology 2015;52:803–18, https://doi.org/10.1177/0300985815588611.
36. Hayami T, Pickarski M, Zhuo Y, Wesolowski GA, Rodan GA, Duong LT. Characterization of articular cartilage and subchondral bone changes in the rat anterior cruciate ligament transection and meniscectomized models of osteoarthritis. Bone 2006;38:234–43, https://doi.org/10.1016/j.bone.2005.08.007.
37. Smith PN, Refshauge KM, Scarvell JM. Development of the concepts of knee kinematics. Arch Phys Med Rehabil 2003;84:1895–902, https://doi.org/10.1016/S0003-9993(03)00281-8.
38. Farrokhi S, Voycheck CA, Klatt BA, Gustafson JA, Tashman S, Fitzgerald GK. Altered tibiofemoral joint contact mechanics and kinematics in patients with knee osteoarthritis and episodic complaints of joint instability. Clin Biomech (Bristol, Avon) 2014;29(6):629–35, https://doi.org/10.1016/j.clinbiomech.2014.04.014.
39. Blaney Davidson EN, van der Kraan PM, van den Berg WB. TGF-β and osteoarthritis. Osteoarthritis Cartilage 2007;15:597–604, https://doi.org/10.1016/j.joca.2007.02.005.

40. Yang X, Chen L, Xu X, Li C, Huang C, Deng CX. TGF-β/Smad3 signals repress chondrocyte hypertrophic differentiation and are required for maintaining articular cartilage. J Cell Biol 2001;153:35–46, https://doi.org/10.1083/jcb.153.1.35.
41. van Beuningen HM, Glansbeek HL, van der Kraan PM, van den Berg WB. Osteoarthritis-like changes in the murine knee joint resulting from intra-articular transforming growth factor-β injections. Osteoarthritis Cartilage 2000;8:25–33, https://doi.org/10.1053/joca.1999.0267.
42. Jacobs BY, Kloefkorn HE, Allen KD. Gait analysis methods for rodent models of osteoarthritis. Curr Pain Headache Rep 2014;18:456, https://doi.org/10.1007/s11916-014-0456-x.